Research Square

Preprints are preliminary reports that have not undergone peer review.
They should not be considered conclusive, used to inform clinical practice,
or referenced by the media as validated information.

Mowing shifts the late-season carbon trajectory without changing the atmospheric control of mid-summer uptake in a temperate meadow steppe

Xiaobo ZHANG

1144796001@qq.com

Gansu Agricultural University

Jingyan Chen

Chinese Academy of Agricultural Sciences

Jiquan Chen

Michigan State University

Xiaoping Xin

Chinese Academy of Agricultural Sciences

Gang Dong

Shanxi University

Shicheng Jiang

Northeast Normal University

Ruirui Yan

Chinese Academy of Agricultural Sciences

Tsegaye Gemechu Legesse

Chinese Academy of Agricultural Sciences

Xiaoni Liu

Gansu Agricultural University

Changliang Shao

Chinese Academy of Agricultural Sciences

Research Article

Keywords: Eddy covariance, Mowing, Vapour pressure deficit, Soil temperature, Temperate meadow steppe

Posted Date: November 25th, 2026

DOI: https://doi.org/10.21203/rs.3.rs-11765071/v1

License: This work is licensed under a Creative Commons Attribution 4.0 International License.
Read Full License

Additional Declarations: No competing interests reported.

Mowing shifts the late-season carbon trajectory without changing the atmospheric control of mid-summer uptake in a temperate meadow steppe

Xiaobo Zhang[1,2,4], Jingyan Chen[2], Jiquan Chen[3], Xiaoping Xin[2], Gang Dong[5], Shicheng Jiang[6], Ruirui Yan[2], Tsegaye Gemechu Legesse[2], Xiaoni Liu[1,4*], Changliang Shao[2*]

[1] Key Laboratory of Grassland Ecosystem, Ministry of Education, Pratacultural College, Gansu Agricultural University

[2] State Key Laboratory of Efficient Utilization of Arable Land in China, National Hulunber Grassland Ecosystem Observation and Research Station, Institute of Agricultural Resources and Regional Planning, Chinese Academy of Agricultural Sciences, Beijing 100081, China

[3] Landscape Ecology & Ecosystem Science, Michigan State University, East Lansing, Michigan, USA

[4] Sino-U.S. Center for Grazing Land Ecosystem Sustainability, Lanzhou, Gansu, China

[5] School of Life Science, Shanxi University, Taiyuan, China

[6] Key Laboratory of Vegetation Ecology, Ministry of Education, Northeast Normal University, Changchun, China

Corresponding author: * Xiaoni Liu liuxn@gsau.edu.cn, *Changliang Shao shaochangliang@caas.cn

Abstract

Background

Temperate grasslands are widely mown for hay, yet it is unclear whether mowing changes only the seasonal trajectory of their carbon exchange or also the environmental controls that shape it. We compared an annually mowed meadow steppe with a fenced control, using one eddy covariance tower per treatment, over 2019-2022.

Results

Both meadow steppes showed a mid-summer depression of gross primary production (GPP) that coincided with the annual maximum in vapour pressure deficit (VPD). Path models gave negative VPD coefficients on GPP in both treatments (-0.35 mowed and -0.29 fenced) and negligible direct coefficients of soil water content, even though the mowed meadow steppe held 14.5-22 percentage points more surface soil water in every year. The fenced meadow steppe was unimodal in all four years, whereas the mowed meadow steppe produced a second late-season maximum in two of four years, in both cases before the harvest date. Growing-season GPP was 31-71% higher in the fenced meadow steppe, and its growing-season carbon sink was 1.3-2.1 times larger; the contrast persisted annually, with a fenced annual sink 1.3-2.9 times that of the mowed meadow steppe in 2019-2022. Soil temperature was the strongest positive control on both GPP and respiration.

Conclusions

Mowing shifted the late-season trajectory and reduced the growing-season carbon sink, but it did not change the atmospheric control of mid-summer uptake or impose a soil-

water constraint at this site. Because each treatment is monitored by one tower, these are site-level contrasts without formal treatment inference, but the annual sink was consistently larger in the fenced meadow steppe in all four years.

Keywords: Eddy covariance; Mowing; Vapour pressure deficit; Soil temperature; Temperate meadow steppe

1. Introduction

Temperate grasslands cover about 32% of the land surface and hold more than 20% of the terrestrial organic carbon pool (Knapp et al., 2008; Soussana et al., 2010; Poulter et al., 2014; Jiang et al., 2025). Their carbon exchange is strongly seasonal, and the shape of that season- when uptake peaks, whether it is interrupted, and how it ends- determines the annual carbon balance (Reichstein et al., 2013; Piao et al., 2020). Most temperate grasslands are managed, and mowing is among the most widespread practices (Soussana et al., 2007; Ding et al., 2021). Whether mowing merely scales the seasonal curve or changes its shape and the controls that produce it is the question addressed here.

A feature common to many temperate grasslands is a mid-summer depression of carbon uptake, when assimilation falls while photosynthetically active radiation (PAR) is near its annual maximum (Flexas et al., 2004; Green et al., 2019). The depression is traditionally attributed to shallow-soil water deficit (Sperry et al., 2002), but atmospheric demand can impose an independent constraint: rising VPD closes stomata to protect the hydraulic system, restricting CO_2 supply even when soil water remains available (Novick et al., 2016; Grossiord et al., 2020; Yuan et al., 2019; Yuan et al., 2025). Separating the two controls is difficult because VPD, temperature and soil moisture covary seasonally, and most evidence comes from unmanaged ecosystems in which the drivers rise and fall together (Humphrey et al., 2021; Xie et al., 2025).

Mowing alters both the canopy and the soil surface. It removes standing biomass and litter, raises soil temperature, and changes interception and transpiration (Wan et al., 2002; Wang et al., 2021; Shi et al., 2022; Liu et al., 2025). These changes can relieve or

aggravate water limitation and can alter the amount and timing of regrowth (Chen et al., 2020; Yan et al., 2023). At our site, mowing raised rather than lowered growing-season soil water content, which separates atmospheric demand from soil water supply- the contrast needed to test whether VPD constrains uptake independently of soil moisture. The two tower sites also differ in soil properties (Additional file 1: Table S3), so the contrast is interpreted at the site level.

We therefore asked three questions: (i) does annual mowing change the shape of the seasonal carbon trajectory; (ii) does it change the relative roles of atmospheric dryness and soil water in constraining GPP; and (iii) what are the consequences for the growing-season carbon budget? We hypothesized that mowing would produce a second late-season maximum in some years (H1), that the mid-summer depression would be driven by VPD rather than soil water in both treatments (H2), and that soil temperature rather than soil water would dominate respiration (H3). Each treatment is monitored by a single tower, so the design yields site-level contrasts and cannot provide replicated treatment inference.

2.Materials and methods

2.1 Study area

The study was conducted at the Changling site (FLUXNET ID CN-Cng; Chen et al., 2019), a meadow steppe on the Songnen Plain, Jilin Province, China (123°30′33″E, 44°35′36″N; 141-171 m a.s.l.). Mean annual temperature is about 5 °C and mean annual precipitation about 400 mm; the water table lies at 1-2 m and the frost-free period lasts 130-165 days. The two towers, CL-MDW (fenced, 44°35′37″N, 123°30′33″E, 141 m) and CL-CLP (mowed, 44°39′01″N, 123°32′15″E, 139 m), are 7-8 km apart on the same

meadow steppe dominated by Leymus chinensis. Mowing was applied once a year at 8 cm stubble height with the herbage removed, on 3 September 2019, 24 October 2020, 5 October 2021 and 8 September 2022.

Soil was described from one profile per tower (five depths to 50 cm). The mowed site has higher surface organic carbon (0-30 cm: 12.2 versus 3.6 g kg^{-1}), total nitrogen (1.6 versus 0.6 g kg-1), silt (54% versus 43%) and available potassium (227 versus 82 mg kg-1), whereas pH (10.1 versus 10.6) and electrical conductivity (512 versus 496 µS cm-1) are similar (Additional file 1: Table S3).

2.2 Flux and micrometeorological measurements

Latent heat (LE), sensible heat (H) and CO_2 fluxes were measured with two open-path eddy covariance systems mounted at 2 m, each combining a CSAT3 sonic anemometer (Campbell Scientific) and an LI-7500 gas analyser (LI-COR) sampling at 10 Hz. Net radiation (CNR4, Kipp & Zonen), PAR (LI-190, LI-COR) and air temperature and humidity (HMP45C, Vaisala) were recorded at 2 m.

Soil temperature at 5 and 10 cm (CS107), soil heat flux at 3 cm (HFT3.1), 0-30 cm water content (CS616) and precipitation (TE-525) were logged as 30-min averages on a CR3000 (all Campbell Scientific).

2.3 Post processing, quality control and gap filling

Half-hourly fluxes were computed in EddyPro 7 with double rotation, cross-correlation lag removal and WPL density correction. Spikes and instrument artefacts were removed, and periods of low turbulence ($u^* < 0.15$ m s^{-1}) were excluded (Chen et al., 2009). Gaps shorter than 2 h were linearly interpolated; longer gaps were filled by marginal

distribution sampling with PAR, VPD and air temperature over windows of ±7, ±14 and ±28 days (Noormets et al., 2007, 2008, 2010).

2.4 Statistical analysis

Analyses used Python 3.11 (NumPy, pandas, scikit-learn) and were checked in SPSS 25; figures used Matplotlib and OriginPro 2024. Probability values are descriptive because the daily series are strongly autocorrelated, and consistency across the four years is treated as the stronger evidence.

The seasonal trajectory was classified mathematically. Daily GPP, Re and NEE were smoothed with a cubic spline, and first and second derivatives were evaluated analytically; a local maximum required a positive-to-negative change in slope and a negative second derivative. A trajectory was unimodal when it had one interior maximum and bimodal when two maxima were separated by a local minimum. The mowed dataset is a continuous daily series; calendar dates were reconstructed from the first observation (15 June 2018) and checked against the seasonal course of air temperature. For Fig. 5 each year was divided into 12 equal relative blocks, which run from the first to the last available observation; the analysis covered 2019-2022 for the mowed meadow steppe and 2018-2023 for the fenced meadow steppe.

Recursive path models were fitted separately to each dataset by standardized least squares. Air and soil temperature are strongly collinear ($r = 0.95$; variance inflation 8.3-12.1), so air temperature entered only the atmospheric equations (VPD, soil water content) and soil temperature only the flux equations (GPP, Re). Standardized coefficients are scale-free and comparable between datasets supplied on different unit bases. The

fenced model uses all days of 2020-2023 while the mowed model uses growing-season days only; Section 3.4 quantifies the effect of this difference.

Random forests (500 trees, minimum five samples per leaf) were fitted separately to each dataset with air temperature, VPD, PAR, soil water content, soil temperature and precipitation as predictors. Partial dependence was evaluated between the 5th and 95th percentiles of each predictor with the others held at their means. Because the temperature variables are collinear, importance scores are treated as descriptive and not as effect sizes.

2.5 Quality control thresholds and flux partitioning

Half-hourly outliers were removed when CO_2 flux exceeded ±20 μmol m^{-2} s^{-1} or when LE or H fell outside -200 to 800 W m^{-2}. Coverage after quality control was 79% for the fenced and 75% for the mowed meadow steppe. Missing data were caused mainly by dew and rain, unfavourable fetch (within ±15° behind the sonic anemometer) and low turbulence.

NEE was partitioned into Re and GPP following Falge et al. (2001) and Reichstein et al. (2005): daytime CO_2 gaps were filled with a light-response equation, and daytime respiration was extrapolated from nighttime temperature-response curves.

Nighttime NEE (PAR < 4 μmol m^{-2} s^{-1}) was modelled against 5-cm soil temperature following Lloyd and Taylor (1994). An apparent Q10 was also estimated for each treatment from positive daily Re and 5-cm soil temperature over May-October (Davidson and Janssens, 2006).

2.6 Energy balance closure

Energy balance closure (EBC) was assessed by regressing turbulent energy (LE + H)

against available energy (Rn - G) at half-hourly resolution using all good data during the growing season (May-October).

The slope was 0.91, 0.80, 0.81 and 0.84 for the fenced meadow steppe in 2020-2023 and 0.82, 0.80, 0.92 and 0.84 for the mowed meadow steppe in 2019-2022 (R^2 = 0.81-0.93). Closure was lowest in 2021 at the fenced tower (0.80) and in 2020 at the mowed tower (0.80), so absolute fluxes of those years are less certain; net radiation is spatially variable and is a major source of closure deficits at eddy covariance sites (Shao et al., 2014).

2.7 Biophysical regulations

Both datasets were split into growing (May-October) and non-growing (November-April) seasons. The constraint analysis uses non-gap-filled half-hourly data, whereas the path models use gap-filled daily data, so the two differ in sample size (n = 635 growing-season days mowed; n = 1,461 days fenced) and are not expected to reproduce one another numerically. Half-hourly fluxes were grouped by air temperature (<15, 15-25, >25 °C), soil water content (<25%, 25-35%, >35%) and VPD (<1, 1-2, >2 kPa); within each group, NEE was binned by PAR in 100 μmol m^{-2} s^{-1} steps and the bin means were fitted with light-response curves (Falge et al., 2001; Li et al., 2005; Zhang et al., 2007).

2.8 Units and comparability of the two flux datasets

The source tables reported both treatments on a CO_2 mass basis, whereas carbon budgets use gC m^{-2}. For the fenced meadow steppe, two overlapping daily files (2018-2022 and 2020-2023) differed by the 44/12 molar-mass ratio over 1,096 common days, showing that one was on a CO_2 basis and the other on a carbon basis; the 2020-2023 file

also gave a plausible water-use efficiency only when read as carbon. All CO_2-basis fluxes were therefore converted by 12/44, so Tables 2 and 4 are on the carbon basis. Because the conversion is a positive constant, it changes magnitudes but not signs or rankings. Table 2 combines the archived mowed series with the processed fenced product: fenced values for 2019-2022 come from the same product used for the annual budgets in Table 4. Where the two fenced products overlap (2020-2022, May-October), they differ by at most 4% in GPP and 1.5% in Re; because NEE is only about one-fifth of GPP, the same gap-filling and partitioning differences amount to 10-16% of NEE without changing signs or rankings.

PAR was a daytime mean at the mowed tower and a 24-h mean at the fenced tower. After conversion to daily integrals the two agreed within 7%, consistent with a May-October daylight fraction of 0.523, so PAR is expressed as a daytime mean for both treatments; identical PAR entries in Table 1 are intentional. The shortwave-radiation column of the fenced file was inconsistent with its PAR column and was not used.

3. Results

3.1. Temporal dynamics of microclimate and subterranean environmental factors

Monitoring covered the full years 2019-2022 at both towers, and the fenced record extends through 2023 (Fig. 1).

Precipitation varied from 323.3 mm in 2019 to 564.9 mm in 2023 (Fig. 1), and precipitation events are an important control on carbon exchange in Inner Mongolian grasslands (Wang et al., 2018). In every growing season the mowed meadow steppe had higher volumetric soil water content (0-30 cm) than the fenced control (e.g., 52.23%

versus 37.73% in 2019 and 59.80% versus 37.72% in 2022; Fig. 1, Table 1). Reduced interception and transpiration after harvest is a plausible but untested explanation; the data do not support accelerated topsoil water loss under mowing.

VPD and PAR followed unimodal seasonal courses with mid-summer maxima above 2.5 kPa and 600 μmol m^{-2} s^{-1} (Fig. 1). Summer topsoil temperature was 2.5-4.5 °C higher under mowing in every year (Table 1), so the two treatments contrast a litter-insulated canopy with a warmer, bare-surface system- a difference that also reflects the soil contrast between the sites (Additional file 1: Table S3).

3.2. Seasonal trajectory of carbon exchange and the mid-summer depression

The shape analysis confirmed that the fenced meadow steppe was unimodal in every year, with a single mid-summer maximum. The mowed meadow steppe produced two maxima separated by a mid-summer depression in 2019 and 2020, but only one maximum in 2021 and 2022 (Fig. 5). The bimodal configuration is therefore recurring but not universal: it was pronounced in two of four mowed years and absent from every fenced year. Because each treatment is represented by one tower, we attach no probability value to this contrast; effect sizes and year-to-year consistency are the evidence.

Both treatments followed the same course until mid-summer. In July, when PAR and air temperature peaked, GPP fell sharply and net uptake flattened in both (Fig. 2), coinciding with the annual VPD maximum (Fig. 1), the pattern expected if atmospheric dryness rather than soil water limits uptake (Section 3.4). After mid-summer the trajectories separated: the fenced meadow steppe recovered gradually to a single broad maximum, whereas the mowed meadow steppe recovered faster and, in two of four years,

produced a second maximum before the end of the growing season. Because harvest dates ranged from 3 September to 24 October, the second maximum occurred before harvest in the years when it was strongest, so post-harvest regrowth cannot be its only cause (Section 4.3).

3.3. Carbon flux magnitudes and seasonal budgets

Fenced GPP exceeded mowed GPP by 31-71% in each year: 460.51 versus 350.23 gC m^{-2} in 2019, 474.27 versus 277.54 in 2020, 521.24 versus 322.17 in 2021 and 554.62 versus 387.68 in 2022. The same direction held for Re (368.58 versus 282.02, 363.95 versus 225.78, 420.44 versus 261.62 and 437.06 versus 332.81 gC m^{-2}) and for the growing-season sink, expressed as negative NEE (91.94 versus 68.22, 110.32 versus 51.75, 100.80 versus 60.55 and 117.56 versus 54.86 gC m^{-2}). Mowed values were computed from the archived daily series, whereas fenced values come from the processed daily product used in Table 4; all values are on the carbon basis; cumulative seasonal trajectories are shown in Additional file 1: Fig. S1. Closure was lowest in 2021 at the fenced tower (0.80) and in 2020 at the mowed tower (0.80), so absolute fluxes of those years are less certain, but the direction of the contrast was consistent in every year; removing 2021 from the fenced series changes its four-year mean GPP by about 1.2% and mean NEE by about 1.4%.

Every non-growing season was a net source in both treatments, releasing 24.57-41.94 gC m^{-2} at the fenced site and 11.54-24.31 gC m^{-2} at the mowed site (Table 4), so the growing-season sink was partly offset by winter losses.

Combining the two seasons, the fenced annual sink was 62.57, 79.27, 76.23 and 75.62 gC m^{-2} yr^{-1} in 2019-2022, 1.3-2.9 times that of the mowed meadow steppe (49.42,

246 27.45, 49.01 and 32.23 gC m^{-2} yr^{-1}); annual mowing therefore reduced the annual carbon
247 sink by 21-65%. Annual GPP was 32-70% higher and annual Re 30-57% higher in the
248 fenced meadow steppe (Table 4). Within the measured growing seasons, the mowed
249 meadow steppe fixed 24-41% less carbon and respired less, and its sink was smaller in
250 every year.

251 **3.4. Environmental controls on carbon exchange**

252 Path models explained 36% and 40% of daily GPP and Re variance in the mowed
253 meadow steppe (n = 635 growing-season days) and 86% of both in the fenced meadow
254 steppe (n = 1,461 days). The two models cover different windows: the fenced model
255 includes four complete years, and the low variance of winter contributes to its higher R2.
256 Refitting both models to the common May-October window with the daily archives
257 reduced the fenced R2 from 0.856 to 0.748 and gave 0.538 for the mowed meadow
258 steppe, narrowing the gap from 0.49 to 0.21; the coefficients of the two refits had the
259 same sign and ranking (fenced: soil temperature +0.586, VPD -0.259, PAR +0.530, soil
260 water content +0.058; mowed: +0.534, -0.318, +0.542 and +0.054). Much of the original
261 difference in fit therefore reflects the seasonal window and the processing of the two
262 archives rather than a different control structure.

263 VPD had a negative coefficient on GPP in both treatments (-0.347 mowed, -0.290
264 fenced) and was the only atmospheric variable with a consistent negative coefficient on
265 Re (-0.267 and -0.251). Entering air and soil temperature with VPD in the GPP equation
266 (Additional file 1: Table S2) kept the VPD coefficient negative (-0.704 and -0.278) and
267 raised variance inflation to 10.6-12.1, so the VPD effect is not an artefact of the

temperature terms. Soil water content had a small direct coefficient on GPP (+0.073 mowed; -0.006, not significant, fenced), and precipitation acted on uptake only through VPD. Soil temperature carried the strongest positive coefficient on both fluxes, larger in the fenced (GPP +0.760, Re +0.950) than in the mowed meadow steppe (GPP +0.434, Re +0.618). PAR was positive for both fluxes in both treatments, and PAR with air temperature explained 57% of VPD variance mowed and 68% fenced. Because the mowed meadow steppe was wetter in every year (Table 1), its soil water content occupied a higher and narrower range (CV 0.24 versus 0.32); this range restriction can attenuate its coefficient, which should be read as an upper bound on any soil-water effect rather than as evidence that none exists.

The apparent Q10 over May-October (n = 736 days per treatment) was 3.22 for the fenced and 1.97 for the mowed meadow steppe, using the same window for both. Excluding 2021, the year of lowest closure at the fenced tower, left the fenced estimate at 2.95. Respiration was therefore more temperature-sensitive where the canopy and litter layer were intact, consistent with moisture-dependent respiration-temperature relationships elsewhere (Seo et al., 2026; Meena et al., 2020).

The random forest (Additional file 1: Fig. S3) reproduced the dominance of soil temperature but also shows why importance is not effect size: in the mowed dataset soil water content ranked second (0.337) behind soil temperature (0.389) despite its small path coefficient (+0.073). Soil water covaries with the seasonal cycle and helps prediction without exerting an independent control; the partial dependence curves are likewise attenuated by temperature collinearity. A de-seasonalized importance ranking would be a

stronger test but was not computed, so inference rests on the path coefficients.

4. Discussion

4.1. Seasonal carbon-exchange trajectory and the role of management

Across four consecutive years, both meadow steppes showed a mid-summer depression of uptake, and the mowed meadow steppe produced a second late-season maximum in two years but not in the other two. The shared depression and the divergent late season are the two results around which the discussion is organized: the first reflects an atmospheric control common to both treatments, the second a management effect on canopy and surface conditions.

4.2. Atmospheric dryness and the origin of the mid-summer depression

The mid-summer depression coincided with the annual VPD maximum in both treatments, and the path models gave a negative VPD coefficient on GPP in both while the direct soil-water coefficient was negligible. Light-response curves under partitioned VPD, temperature and soil water (Fig. 3) point the same way: at VPD above 2 kPa the light-saturated uptake was lower in both treatments.

The mechanism is stomatal. Rising VPD increases the leaf-to-air vapour-pressure gradient; to avoid xylem cavitation the vegetation closes stomata, which restricts CO_2 supply even when PAR and temperature are near their optima (Sperry et al., 2002; Grossiord et al., 2020; Li et al., 2025; Lin et al., 2025). This interpretation does not require soil water to be limiting, and at our site it was not: the mowed meadow steppe was wetter than the fenced control in every year, yet showed the same VPD signal.

Two checks support this reading. Entering air and soil temperature alongside VPD left the

VPD coefficient negative and raised the variance inflation factors only to 10.6-12.1, so the atmospheric effect is not a proxy for temperature (Additional file 1: Table S2). The random forest, which makes no assumption about pathway structure, also ranked soil temperature first, with soil water contributing to prediction through its seasonal covariation rather than as an independent constraint. The negative VPD coefficient on Re is consistent with substrate limitation: stomatal closure lowers assimilation, and the smaller supply of recent photosynthate lowers respiration.

A caveat applies to the soil-water conclusion: water content was measured over 0-30 cm, whereas Leymus chinensis roots extend below this layer above a water table at 1-2 m. The absence of a soil-water constraint therefore applies to the measured surface layer, not necessarily to the whole root zone.

4.3. Late-season recovery in the mowed meadow steppe: evidence and alternative mechanisms

The clearest divergence was the late-season maximum in the mowed meadow steppe in 2019 and 2020. It was weak or absent in 2021 and 2022, so the mechanism below explains a recurring but non-universal pattern rather than an established process. After the VPD maximum, the recovery slope of NEE against temperature and moisture was steeper in the mowed plot (Additional file 1: Fig. S2), consistent with a greater recovery capacity but not proof of compensatory regrowth (Reichstein et al., 2013). The path models describe a control structure, not a causal chain, and biomass and leaf area were not measured.

Compensatory regrowth is one candidate mechanism, inferred rather than measured:

removal of the canopy can release buds and carbohydrate reserves, and new tissues can have higher carboxylation and light-use capacity than senescent mid-summer tissue (Chen et al., 2020; Yan et al., 2023; Koncz et al., 2017). Two alternatives cannot be separated with these data: a carry-over effect of the previous autumn's harvest on spring phenology and canopy structure, and litter removal raising spring soil temperature and advancing green-up. Because the second maximum occurred before harvest in the years when it was strongest, post-harvest regrowth alone cannot explain it.

The control structure offers a second, non-biological reason for faster late-season recovery. Assimilation and respiration were both limited mainly by soil temperature, and that limitation was weaker in the mowed meadow steppe, so a given relaxation of atmospheric demand released a larger proportional gain in uptake than in respiratory loss. The data cannot separate this from a direct effect of defoliation on canopy development.

4.4. Soil hydrothermal controls and the respiration balance under mowing

Mowing was associated with a different configuration of the belowground controls. In the fenced meadow steppe, soil water content varied mainly with atmospheric demand: the path model gives -0.428 from VPD to soil water, with air temperature acting only through VPD. That coupling is consistent with the hydro-insulating effect of a well-developed litter layer, inferred from the literature because litter mass was not measured here. Under mowing, soil water content was 14.5-22 percentage points higher in every growing season, consistent with reduced transpiration and interception after harvest. The mowed site also has finer texture and higher organic carbon (Additional file 1: Table S3), which may contribute to its greater water retention, so the difference cannot be attributed to

356 mowing alone. In either case, the additional water had only a small direct coefficient on
357 uptake (+0.073 mowed; -0.006 fenced).

358 Soil temperature exerted a positive and significant control on Re in both treatments,
359 stronger in the fenced (+0.950) than in the mowed meadow steppe (+0.618). Warmer soil
360 therefore does not by itself explain the mowed carbon balance, and growing-season Re
361 was lower under mowing in every year. The lower apparent Q10 (1.97 versus 3.22),
362 together with the lower measured respiration, suggests that reduced substrate and
363 respiring biomass outweighed the direct effect of warmer soil; respiration in meadow and
364 steppe soils also responds strongly to seasonal moisture and temperature (Tomar and
365 Baishya, 2020; Kang et al., 2024).

366 Taken together, the two datasets describe a system in which soil temperature governs
367 both uptake and release, in which soil water is not an independent constraint on
368 assimilation, and in which the growing-season balance depends on how much of the
369 season carries an active canopy. Warmth and moisture in the mowed topsoil did not
370 produce a respiratory penalty: Re was lower under mowing in every year, indicating that
371 reduced respiring biomass outweighed the temperature increase. The growing-season
372 carbon cost of mowing is therefore consistent with the period of reduced canopy cover
373 after harvest rather than with accelerated belowground metabolism.

374 These findings do not establish a management prescription. If the late-season
375 recovery is reproduced elsewhere, timely mowing might support forage production and
376 late-season uptake where autumn water supply is adequate; where autumn drought
377 intensifies, that benefit could be offset by water limitation. Replicated towers and harvest-

timing experiments are required before such possibilities can guide management.

4.5. Comparison with published defoliation experiments

The direction of the mowing effect differs among published studies (Additional file 1: Table S1). In a temperate sown meadow steppe in France, mowing left gross productivity unchanged and reduced Re relative to grazing, so the mowed system was the stronger sink (-476 versus -231 gC m^{-2} yr^{-1}; Senapati et al., 2014). In sandy meadow steppes in Hungary the opposite occurred: mowing lowered GPP by 8% and raised Re by 4%, turning a sink into a source (Koncz et al., 2017), and the same site gave +1.0 versus -0.3 t C ha^{-1} yr^{-1} under grazing and mowing, respectively (Koncz et al., 2020). Our mowed meadow steppe remained a growing-season sink, placing it closer to the French than to the Hungarian case.

Two factors plausibly explain the spread. The first is water supply: the Hungarian site is a semi-arid sandy meadow steppe where soil water limits production, and mowing lowered the annual balance most strongly in the driest year (Koncz et al., 2017). Clipping experiments in tallgrass prairie show that defoliation warms the surface by 3.4-4.3 °C and lowers soil moisture by 18-23% (Wan et al., 2002); with a shallow water table, as at our site, that loss is smaller and the carbon cost correspondingly lower. The second is the litter layer: litter removal raised PAR at the soil surface by about 30% and increased NEP by 23.9% over seven years in a Mongolian steppe, whereas litter addition raised Re by 14.9% without changing NEP (Wang et al., 2021). A canopy and litter layer is therefore not unambiguously beneficial, which weakens the assumption that removing it must impose a carbon cost.

The published systems also differ in mowing regime. Our treatment was cut once annually to 8 cm with the herbage removed, whereas the Hungarian and French studies differ in frequency, stubble height and residue management; these differences are confounded with climate in any cross-site comparison. Post-drought regrowth recovered 39% of the preceding loss at plot scale and 11-17% at landscape and regional scales in a Tibetan alpine grassland (Chen et al., 2020), so late-season recovery has precedent in these systems.

Several limitations qualify these inferences. First, each treatment is monitored by a single tower, so the contrast is a site-level difference without replication. Second, the two tower sites differ in soil properties (0-30 cm SOC 3.6 versus 12.2 g kg^{-1}, silt 43% versus 54%; Additional file 1: Table S3), so part of the hydrological contrast may be site rather than management. Third, the mowed calendar dates were reconstructed from a continuous daily record rather than logged directly, so the timing of the second maximum carries some uncertainty relative to the harvest dates. Fourth, biomass, leaf area and litter mass were not measured, so the compensatory-regrowth and litter-insulation mechanisms remain inferred. Fifth, the path models for the two treatments cover different seasonal windows. Finally, closure was lowest in 2021 at the fenced tower (0.80) and in 2020 at the mowed tower (0.80), so absolute fluxes of those years are less certain.

5. Conclusion

In a temperate meadow steppe, annual mowing shifted the late-season carbon trajectory and reduced the growing-season carbon sink, but it did not change the atmospheric control of mid-summer uptake. Both treatments showed a mid-summer depression tied to VPD,

and soil water did not constrain GPP even where mowing raised it. A second late-season maximum appeared in two of four mowed years and was absent from the fenced control; the data support a conditional association with compensatory regrowth. Soil temperature was the strongest control on respiration, and growing-season respiration was lower under mowing. The non-growing season was a net source in both treatments, and the fenced annual sink was 1.3-2.9 times that of the mowed meadow steppe in 2019-2022.

Acknowledgements

This study was supported by the National Key Research and Development Program of China (2024YFE0198604, 2021YFD1300500), and the Natural Science Foundation of China (32192464). We gratefully acknowledge the Special Funding for Modern Agricultural Technology Systems from the Chinese Ministry of Agriculture, the China Agriculture Research System (CARS-34), and the technical support from USCCC and ChinaFLUX.

Declarations

Ethics approval and consent to participate

Not applicable.

Consent for publication

Not applicable.

Availability of data and material

The datasets generated and analysed during the current study are available from the corresponding author on reasonable request.

Competing interests

The authors declare that they have no competing interests.

Funding

This study was supported by the National Key Research and Development Program of China (2024YFE0198604 and 2021YFD1300500), the Natural Science Foundation of China (32192464), the Special Funding for Modern Agricultural Technology Systems from the Chinese Ministry of Agriculture, and the China Agriculture Research System (CARS-34).

Authors' contributions

X.B.Z. and C.L.S. conceived and designed the study. X.B.Z., J.Y.C., S.C.J., and T.G.L. collected, processed, and curated the data. X.B.Z., and J.Y.C. conducted the analyses and prepared the figures and tables. X.B.Z. wrote the initial manuscript. J.Q.C., X.P.X., G.D., R.R.Y., X.N.L., and C.L.S. reviewed and revised the manuscript. X.N.L. and C.L.S. supervised the project and acquired funding. All authors reviewed and approved the final manuscript and agree to be accountable for all aspects of the work.

Acknowledgements

The authors thank the USCCC and ChinaFLUX for technical support.

Authors' information (optional)

The corresponding authors of this article are Xiaobo Zhang (144796001@qq.com), Xiaoni Liu (liuxn@gsau.edu.cn), and Changliang Shao (shaochangliang@caas.cn). Xiaobo Zhang is affiliated with the Pratacultural College, Gansu Agricultural University, Lanzhou, Gansu, China, and with the Institute of Agricultural Resources and Regional Planning, Chinese Academy of Agricultural Sciences, Beijing, China. Xiaoni Liu is

affiliated with the Key Laboratory of Grassland Ecosystem, Ministry of Education, Pratacultural College, Gansu Agricultural University, and with the Sino-U.S. Center for Grazing Land Ecosystem Sustainability, Lanzhou, Gansu, China. Changliang Shao is affiliated with the State Key Laboratory of Efficient Utilization of Arable Land in China and the National Hulunber Grassland Ecosystem Observation and Research Station, Institute of Agricultural Resources and Regional Planning, Chinese Academy of Agricultural Sciences, Beijing, China. The authors collaborate on research into carbon and water exchange and ecosystem management in temperate grasslands of northern China, with a focus on long-term eddy covariance observations in the Hulunber meadow steppe.

References

Chen JY, Shao CL, Jiang SC et al (2019) Effects of changes in precipitation on energy and water balance in a Eurasian meadow steppe. Ecol Process 8:17 https://doi.org/10.1186/s13717-019-0170-z

Chen N, Zhang YJ, Zu JX et al (2020) The compensation effects of post-drought regrowth on earlier drought loss across the tibetan plateau grasslands. Agric For Meteorol 281:107822 https://doi.org/10.1016/j.agrformet.2019.107822

Chen S, Chen J, Lin G et al (2009) Energy balance and partition in Inner Mongolia steppe ecosystems with different land use types. Agric For Meteorol 149:1800–1809 https://doi.org/10.1016/j.agrformet.2009.06.009

Davidson EA, Janssens IA (2006) Temperature sensitivity of soil carbon decomposition and feedbacks to climate change. Nature 440:165–173

https://doi.org/10.1038/nature04514

Ding C, Yang G, Wang X et al (2021) Mowing weakens the positive effects of nitrogen deposition on fundamental ecosystem service of grassland. Ecol Process 10:2 https://doi.org/10.1186/s13717-020-00273-2

Falge E, Baldocchi D, Olson R et al (2001) Gap filling strategies for defensible annual sums of net ecosystem exchange. Agric For Meteorol 107:43–69 https://doi.org/10.1016/s0168-1923(00)00225-2

Flexas J, Bota J, Loreto F et al (2004) Diffusive and metabolic limitations to photosynthesis under drought and salinity in C3 plants. Plant Biol 6:269–279 https://doi.org/10.1055/s-2004-820867

Green JK, Seneviratne SI, Berg AM et al (2019) Large influence of soil moisture on long-term terrestrial carbon uptake. Nature 565:476 https://doi.org/10.1038/s41586-018-0848-x

Grossiord C, Buckley TN, Cernusak LA et al (2020) Plant responses to rising vapor pressure deficit. New Phytol 226:1550–1566 https://doi.org/10.1111/nph.16485

Humphrey V, Berg A, Ciais P et al (2021) Soil moisture-atmosphere feedback dominates land carbon uptake variability. Nature 592:65 https://doi.org/10.1038/s41586-021-03325-5

Jiang Z, Ma H, Li S et al (2025) Towards smart soil carbon pool management of grassland: a bibliometric overview from past to future. Ecol Process 14:54 https://doi.org/10.1186/s13717-025-00620-1

Kang X, Liu T, Hao L et al (2024) Understanding soil and ecosystem respiration in a

510 dune-meadow cascade ecosystem. Ecol Process 13:81
511 https://doi.org/10.1186/s13717-024-00557-x
512 Knapp AK, Beier C, Briske DD et al (2008) Consequences of more extreme precipitation
513 regimes for terrestrial ecosystems. Bioscience 58:811–821
514 Koncz P, Pintér K, Balogh J et al (2017) Extensive grazing in contrast to mowing is
515 climate-friendly based on the farm-scale greenhouse gas balance. Agric Ecosyst
516 Environ 240:121–134 https://doi.org/10.1016/j.agee.2017.02.022
517 Koncz P, Vadász-Besnyoi V, Csathó AI et al (2020) Carbon uptake changed but vegetation
518 composition remained stable during transition from grazing to mowing grassland
519 management. Agric Ecosyst Environ 304:107161
520 https://doi.org/10.1016/j.agee.2020.107161
521 Li F, Xin Q, Yi C et al (2025) Limited regulation of canopy water use efficiency by
522 stomatal behavior under drought propagation. Glob Chang Biol 31:e70381
523 https://doi.org/10.1111/gcb.70381
524 Lin SR, Chen XZ, Xia JZ et al (2025) Global vegetation production may decrease in this
525 century due to rising atmospheric dryness. Nat Ecol Evol 9:2279–2289
526 https://doi.org/10.1038/s41559-025-02885-3
527 Li SG, Asanuma J, Eugster W et al (2005) Net ecosystem carbon dioxide exchange over
528 grazed steppe in central Mongolia. Glob Chang Biol 11:1941–1955
529 https://doi.org/10.1111/j.1365-2486.2005.01047.x
530 Liu H, Ren F, Wan S et al (2025) Nitrogen and water additions with or without mowing
531 altered soil microbial community characteristics in a semi-arid steppe. Ecol Process

14:3 https://doi.org/10.1186/s13717-024-00568-8

Lloyd J, Taylor JA (1994) On the temperature dependence of soil respiration. Funct Ecol 8:315–323 https://doi.org/10.2307/2389824

Meena A, Hanief M, Dinakaran J et al (2020) Soil moisture controls the spatio-temporal pattern of soil respiration under different land use systems in a semi-arid ecosystem of Delhi, India. Ecol Process 9:15 https://doi.org/10.1186/s13717-020-0218-0

Noormets A, Chen J, Crow TR (2007) Age-dependent changes in ecosystem carbon fluxes in managed forests in northern wisconsin, USA. Ecosystems 10:187–203 https://doi.org/10.1007/s10021-007-9018-y

Noormets A, Gavazzi MJ, McNulty SG et al (2010) Response of carbon fluxes to drought in a coastal plain loblolly pine forest. Glob Chang Biol 16:272–287 https://doi.org/10.1111/j.1365-2486.2009.01928.x

Noormets A, McNulty SG, DeForest JL et al (2008) Drought during canopy development has lasting effect on annual carbon balance in a deciduous temperate forest. New Phytol 179:818–828 https://doi.org/10.1111/j.1469-8137.2008.02501.x

Novick KA, Ficklin DL, Stoy PC et al (2016) The increasing importance of atmospheric demand for ecosystem water and carbon fluxes. Nat Clim Chang 6:1023–1027 https://doi.org/10.1038/nclimate3114

Piao S, Wang X, Park T et al (2020) Characteristics, drivers and feedbacks of global greening. Nat Rev Earth Environ 1:14–27

Poulter B, Frank D, Ciais P et al (2014) Contribution of semi-arid ecosystems to interannual variability of the global carbon cycle. Nature 509:600

554 Reichstein M, Bahn M, Ciais P et al (2013) Climate extremes and the carbon cycle.
555 Nature 500:287–295
556 Reichstein M, Falge E, Baldocchi D et al (2005) On the separation of net ecosystem
557 exchange into assimilation and ecosystem respiration: review and improved
558 algorithm. Glob Chang Biol 11:1424–1439 https://doi.org/10.1111/j.1365-
559 2486.2005.001002.x
560 Senapati N, Chabbi A, Gastal F et al (2014) Net carbon storage measured in a mowed and
561 grazed temperate sown grassland shows potential for carbon sequestration under
562 grazed system. Carbon Manag 5:131–144
563 https://doi.org/10.1080/17583004.2014.912863
564 Seo D, Lee M, Lee J et al (2026) Greater moisture dependence of the soil respiration
565 response to temperature under relatively lower soil moisture conditions in a
566 temperate deciduous broadleaved forest. Ecol Process 15:94
567 https://doi.org/10.1186/s13717-026-00752-y
568 Shao C, Li L, Dong G et al (2014) Spatial variation of net radiation and its contribution to
569 energy balance closures in grassland ecosystems. Ecol Process 3:7
570 https://doi.org/10.1186/2192-1709-3-7
571 Shi LA, Lin ZR, Tang SM et al (2022) Interactive effects of warming and managements
572 on carbon fluxes in grasslands: A global meta-analysis. Agric Ecosyst Environ
573 340:108178 https://doi.org/10.1016/j.agee.2022.108178
574 Soussana JF, Allard V, Pilegaard K et al (2007) Full accounting of the greenhouse gas
575 (CO_2, N_2, CH_4) budget of nine European grassland sites. Agric Ecosyst Environ

121:121–134

Soussana JF, Tallec T, Blanfort V (2010) Mitigating the greenhouse gas balance of ruminant production systems through carbon sequestration in grasslands. Animal 4:334–350 https://doi.org/10.1017/s1751731109990784

Sperry JS, Hacke UG, Oren R et al (2002) Water deficits and hydraulic limits to leaf water supply. Plant Cell Environ 25:251–263 https://doi.org/10.1046/j.0016-8025.2001.00799.x

Tomar U, Baishya R (2020) Seasonality and moisture regime control soil respiration, enzyme activities, and soil microbial biomass carbon in a semi-arid forest of Delhi, India. Ecol Process 9:50 https://doi.org/10.1186/s13717-020-00252-7

Wang J, Zhang A, Zheng YJ et al (2021) Long-term litter removal rather than litter addition enhances ecosystem carbon sequestration in a temperate steppe. Funct Ecol 35:2799–2807 https://doi.org/10.1111/1365-2435.13920

Wang Y, Chen JQ, Zhou GS et al (2018) Predominance of precipitation event controls ecosystem CO2 exchange in an Inner Mongolian desert grassland, China. J Clean Prod 197:781–793 https://doi.org/10.1016/j.jclepro.2018.06.107

Wan S, Luo Y, Wallace LL (2002) Changes in microclimate induced by experimental warming and clipping in tallgrass prairie. Glob Chang Biol 8:754–768 https://doi.org/10.1046/j.1365-2486.2002.00510.x

Xie H, Tian S, Li F et al (2025) Contrasting diurnal impacts of vapor pressure deficit on water use efficiency in two semiarid steppe ecosystems. Ecol Process 14:68 https://doi.org/10.1186/s13717-025-00636-7

598 Yan Y, Quan Q, Wang J et al (2023) Clipping increases ecosystem carbon use efficiency
599 by decreasing the dominance of grasses. Agric For Meteorol 334:109421
600 https://doi.org/10.1016/j.agrformet.2023.109421
601 Yuan WP, Tian J, Wang M et al (2025) Impacts of rising atmospheric dryness on
602 terrestrial ecosystem carbon cycle. Nat Rev Earth Environ 6:712–727
603 https://doi.org/10.1038/s43017-025-00726-2
604 Yuan W, Zheng Y, Piao S et al (2019) Increased atmospheric vapor pressure deficit
605 reduces global vegetation growth. Sci Adv 5: eaax1396
606 Zhang WL, Chen SP, Chen J et al (2007) Biophysical regulations of carbon fluxes of a
607 steppe and a cultivated cropland in semiarid Inner Mongolia. Agric For Meteorol
608 146:216–229 https://doi.org/10.1016/j.agrformet.2007.06.002
609

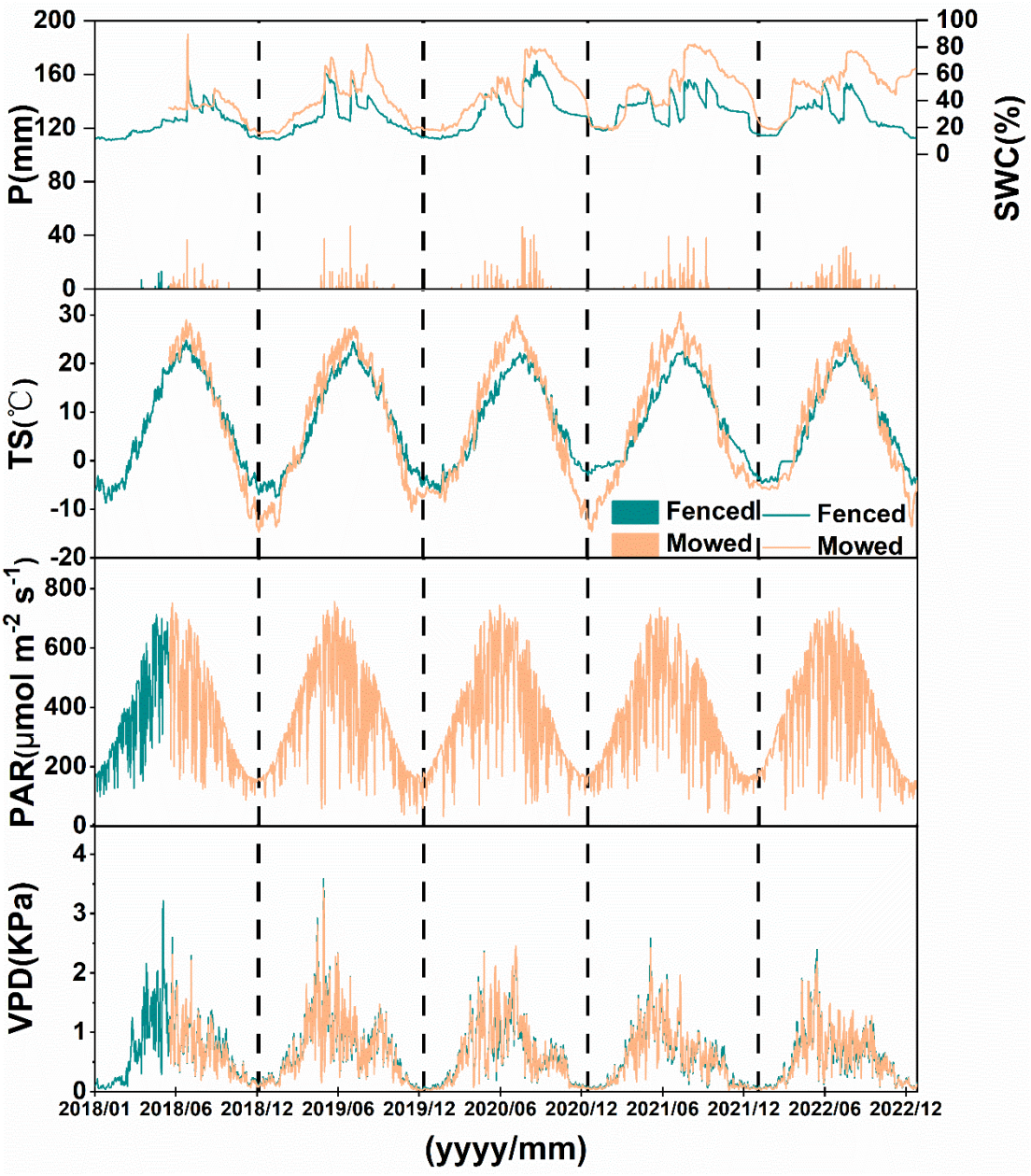

Figure 1. Multi-year time-series profiles of macroscopic microclimatic drivers and topsoil hygrothermal dynamics under fenced and mowed management regimes. The fenced dataset covers 2020 to 2023 and the mowed dataset the growing seasons of 2019 to 2022.

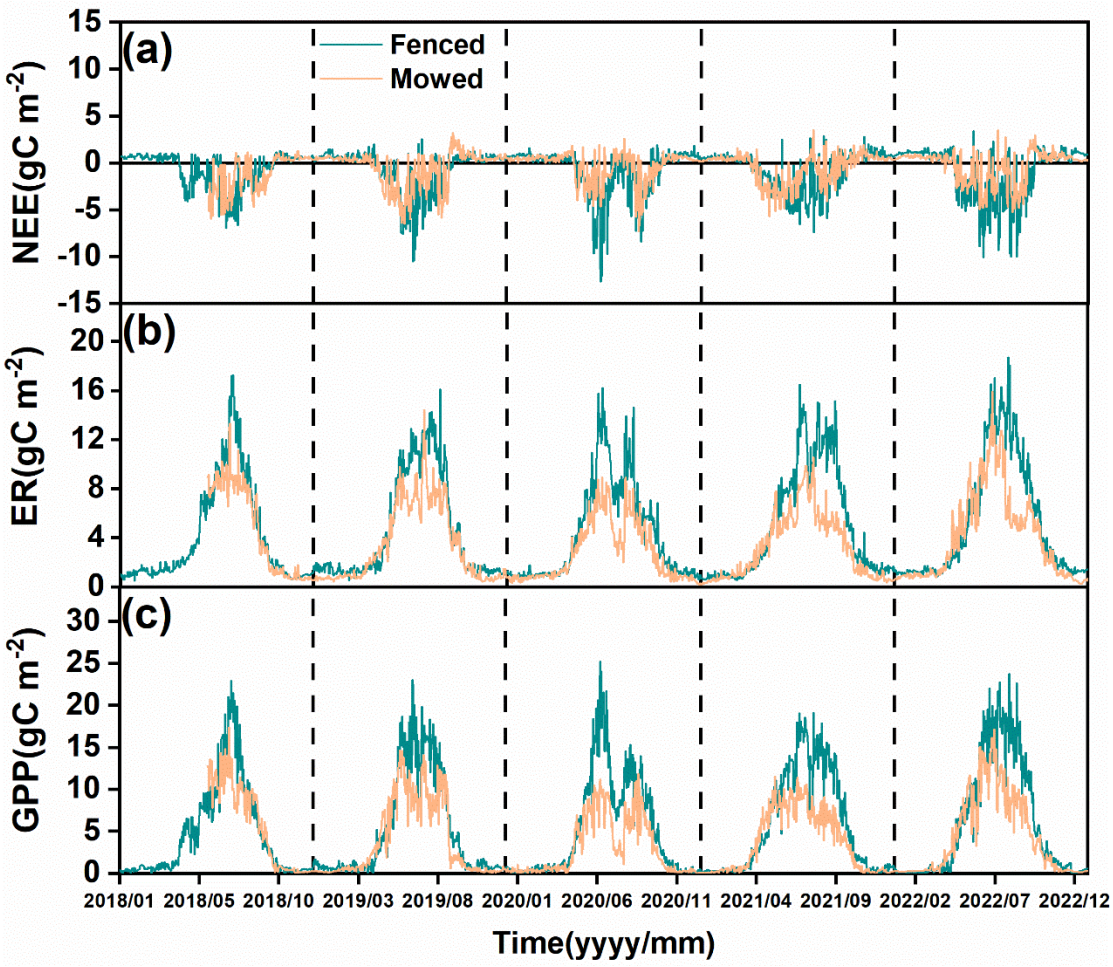

Figure 2. Seasonal trajectories of daily NEE, ER, and GPP distinguishing the physiological carbon dynamics between fenced and mowed meadow steppes. The fenced dataset covers 2020 to 2023 and the mowed dataset the growing seasons of 2019 to 2022.

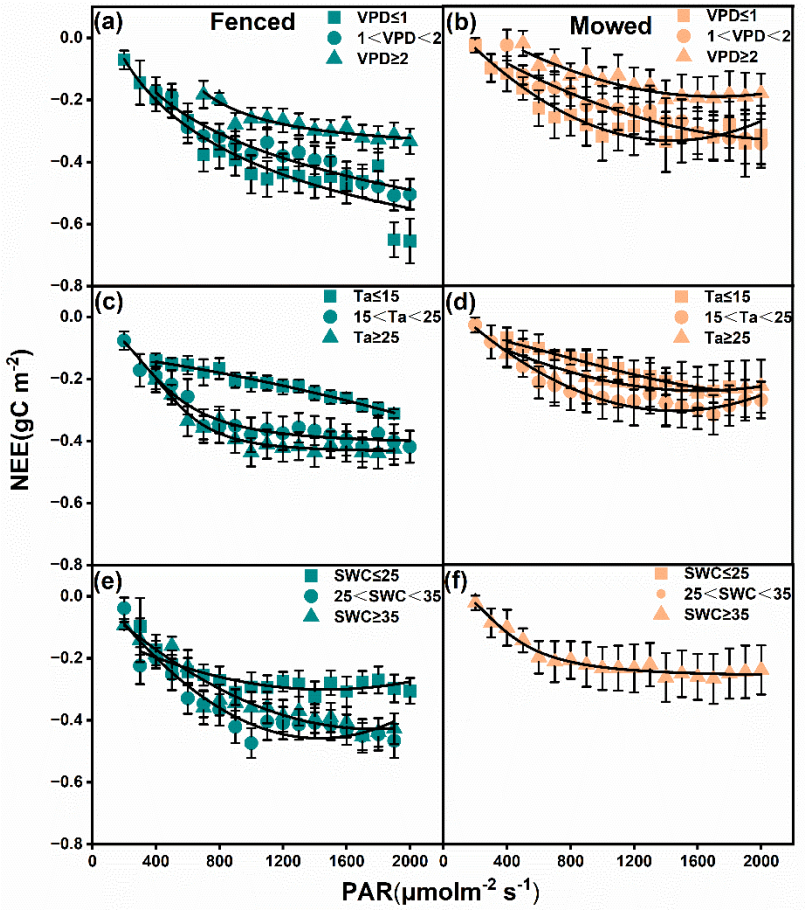

621

622 **Figure 3. Light-response curves of daily NEE under partitioned gradients of VPD, Ta,**

623 **and SWC for fenced and mowed meadow steppes.**

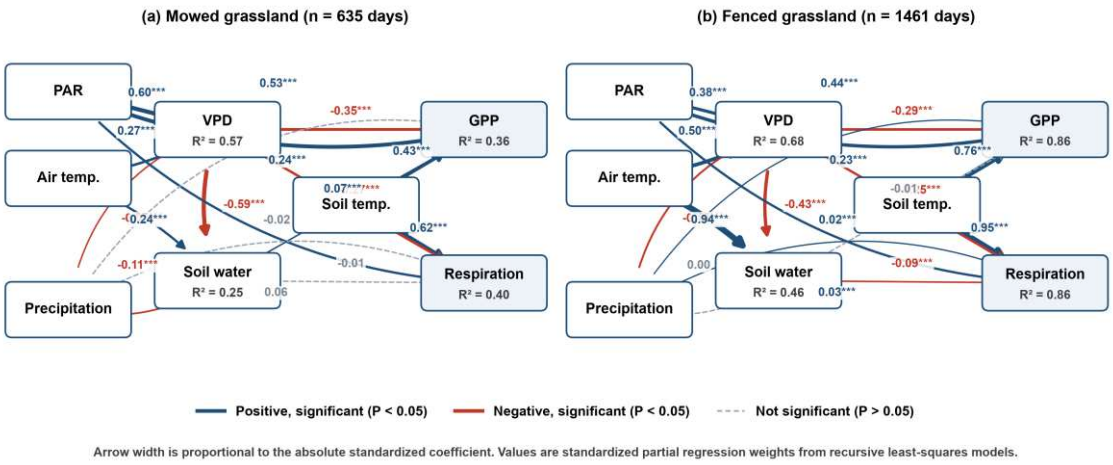

624

625 **Figure 4. Standardized path diagram of the environmental controls on gross primary**

626 **production and ecosystem respiration in (a) the mowed meadow steppe and (b) the**

627 **fenced meadow steppe. Arrow width is proportional to the absolute standardized**

coefficient; blue arrows are positive and significant, red arrows negative and significant, and dashed grey arrows are not significant (P > 0.05). Values in boxes are the proportion of variance explained. Air temperature enters only the atmospheric equations and soil temperature only the flux equations, so no equation contains two collinear temperature variables. Coefficients are rounded to two decimals.

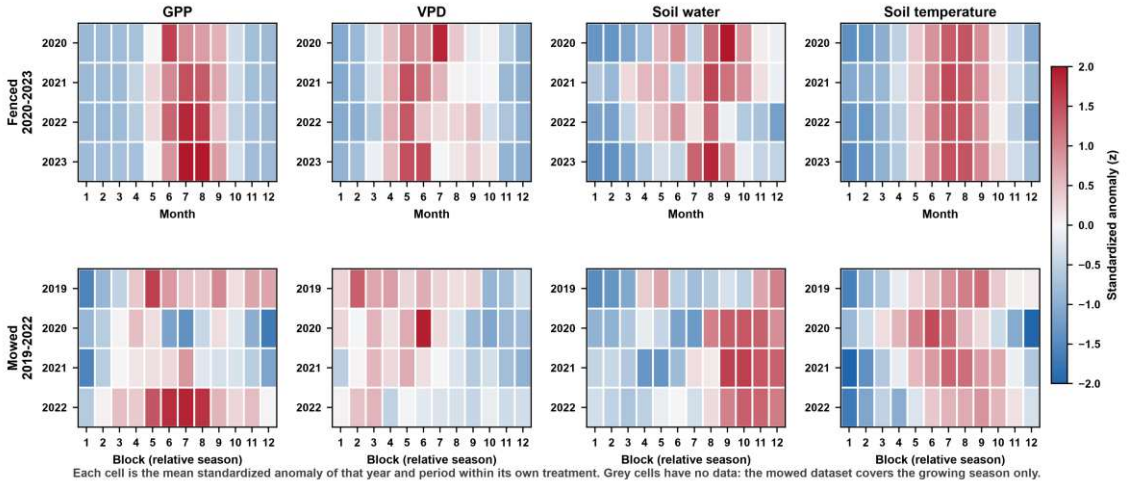

Figure 5. Year-by-period standardized anomalies of gross primary production, vapour pressure deficit, soil water content and soil temperature. The upper row shows the fenced meadow steppe by calendar month (2020-2023). The lower row shows the mowed meadow steppe by relative seasonal block within each labelled year (2019-2022); the source is a continuous daily series whose calendar dates were reconstructed from the first observation (15 June 2018), and the 12 blocks divide each year from the first to the last available observation. Each cell is the mean anomaly of that period within its own treatment; grey cells have no data. The two rows are not on a common calendar axis and are not aligned in time.

Table 1. Growing-season microclimate and topsoil conditions in the fenced (F) and

mowed (M) meadow steppes, 2019-2022

Parameter	2019 F	2019 M	2020 F	2020 M	2021 F	2021 M	2022 F	2022 M
PPT (mm)	323.3	323.3	458.7	458.7	429.8	429.8	441.8	441.8
SWC (%)	37.73	52.23	42.66	57.58	38.62	58.26	37.72	59.80
Tair (°C)	20.55	20.37	19.42	19.49	18.48	18.48	19.67	20.13
Ts (°C)	17.57	20.11	16.38	20.03	15.13	19.60	16.31	18.83
PAR (µmol m^{-2} s^{-1})	484.32	484.32	454.85	454.85	455.54	455.54	491.06	491.06
VPD (kPa)	1.04	1.07	0.90	0.95	0.86	0.87	0.85	0.88

Table 1 legend. Growing-season (May-October) totals of precipitation (PPT), volumetric soil water content over 0-30 cm (SWC), air temperature at 2 m (Tair), soil temperature at 5 cm (Ts), photosynthetically active radiation (PAR) and vapour pressure deficit (VPD) for the fenced (F) and mowed (M) meadow steppes, 2019-2022. SWC is expressed as a percentage of soil volume and is high for a steppe soil because the site overlies a water table at 1-2 m. PAR is a daytime mean from the mowed tower applied to both treatments (Section 2.8), so identical entries are intentional. Precipitation is from the tower-based records and is common to both treatments. Values are rounded.

Table 2. Growing-season carbon budget of the fenced and mowed meadow steppes, 2019-2022

Year	Fenced meadow steppe			Mowed meadow steppe		
	GPP	Re	NEE	GPP	Re	NEE
2019	460.51	368.58	-91.94	350.23	282.02	-68.22
2020	474.27	363.95	-110.32	277.54	225.78	-51.75
2021	521.24	420.44	-100.80	322.17	261.62	-60.55
2022	554.62	437.06	-117.56	387.68	332.81	-54.86

Table 2 legend. Growing-season (May-October) totals in gC m^{-2} on the carbon basis (Section 2.8); mowed values come from the archived daily series, and fenced values from the processed daily product used in Table 4. Negative NEE denotes a net carbon sink. Non-growing-season and

annual values for both treatments are given in Table 4.

Table 3. Standardized path coefficients for the mowed and fenced meadow steppe

Path	Mowed meadow steppe	Fenced meadow steppe
Air temperature to VPD	0.275 ***	0.501 ***
PAR to VPD	0.596 ***	0.383 ***
Precipitation to VPD	-0.075 ***	-0.161 ***
R squared of the VPD model	0.565	0.678
Air temperature to soil water content	0.236 ***	0.936 ***
VPD to soil water content	-0.594 ***	-0.428 ***
Precipitation to soil water content	-0.114 ***	0.003 ns
R squared of the soil water content model	0.253	0.460
Soil temperature to GPP	0.434 ***	0.760 ***
VPD to GPP	-0.347 ***	-0.290 ***
PAR to GPP	0.531 ***	0.436 ***
Soil water content to GPP	0.073 ***	-0.006 ns
Precipitation to GPP	-0.019 ns	0.021 ***
R squared of the GPP model	0.363	0.856
Soil temperature to respiration	0.618 ***	0.950 ***
VPD to respiration	-0.267 ***	-0.251 ***
PAR to respiration	0.237 ***	0.233 ***
Soil water content to respiration	-0.012 ns	-0.090 ***
Precipitation to respiration	0.057 ns	0.033 ***
R squared of the respiration model	0.397	0.858

Table 3 legend. Standardized path coefficients of the recursive models fitted separately to the mowed and the fenced meadow steppe. Coefficients are fully standardized partial regression weights, and the R squared rows give the proportion of variance explained by each equation. Asterisks denote significance (* P < 0.001, ** P < 0.01, * P < 0.05); ns = not significant. The fenced model is fitted to all days of 2020-2023; refitting both models to the common May-October window with the daily archives gives R^2 = 0.748 for the fenced and 0.538 for the mowed meadow steppe, with coefficients of the same sign and ranking (Section 3.4).**

Table 4. Non-growing-season and annual carbon budget of the fenced and mowed meadow steppes, 2019-2022

Treatment	Period	Year	Days	NEE	Re	GPP
Fenced	**Non-growing season**	2019	181	29.36	68.17	38.80
Fenced	**Non-growing season**	2020	182	31.05	56.76	25.71
Fenced	**Non-growing season**	2021	181	24.57	64.15	39.58
Fenced	**Non-growing season**	2022	181	41.94	71.83	29.89
Fenced	**Annual**	2019	365	-62.57	436.74	499.32
Fenced	**Annual**	2020	366	-79.27	420.71	499.98
Fenced	**Annual**	2021	365	-76.23	484.59	560.82
Fenced	**Annual**	2022	365	-75.62	508.90	584.52
Mowed	**Non-growing season**	2019	181	18.80	46.28	27.48
Mowed	**Non-growing season**	2020	182	24.31	41.77	17.46
Mowed	**Non-growing season**	2021	181	11.54	53.20	41.66
Mowed	**Non-growing season**	2022	181	22.63	59.35	36.72
Mowed	**Annual**	2019	365	-49.42	328.30	377.72
Mowed	**Annual**	2020	366	-27.45	267.55	295.00
Mowed	**Annual**	2021	365	-49.01	314.82	363.83
Mowed	**Annual**	2022	365	-32.23	392.16	424.39

Table 4 legend. Non-growing-season and annual carbon budget of the fenced and mowed meadow steppes, 2019-2022. The non-growing season (N-GS) November to April; annual rows are the sums of the two seasons. NEE, Re and GPP are in g C m^{-2} for the period indicated. Negative NEE denotes a net carbon sink and positive NEE a net source. Both treatments cover 2019-2022, so the annual comparison uses all four years. Growing-season totals are given in Table 2; each annual row is the sum of the growing-season total (Table 2) and the non-growing-season value.